arXiv:2102.05795v1 [astro-ph.HE] 11 Feb 2021

# FIRST J153350.8+272729: the radio afterglow of a decades-old tidal disruption event

Vikram Ravi,[1] Hannah Dykaar,[2,3] Jackson Codd,[4,5] Ginevra Zaccagnini,[4] Dillon Dong,[1] Maria R. Drout,[2,6] B. M. Gaensler,[3,2] Gregg Hallinan,[1] and Casey Law[1]

[1]Cahill Center for Astronomy and Astrophysics, California Institute of Technology, Pasadena, CA 91125, USA
[2]David A. Dunlap Department of Astronomy and Astrophysics, University of Toronto
50 St. George Street, Toronto, Ontario, M5S 3H4 Canada
[3]Dunlap Institute for Astronomy and Astrophysics, University of Toronto, 50 St. George St., Toronto, ON M5S 3H4, Canada
[4]Cambridge Rindge and Latin School, Cambridge, MA, USA
[5]Department of Physics, Macalester College, Saint Paul, MN 55105, USA
[6]Observatories of the Carnegie Institution for Science, 813 Santa Barbara St., Pasadena, CA 91101, USA

## ABSTRACT

We present the discovery of the fading radio transient FIRST J153350.8+272729. The source had a maximum observed 5-GHz radio luminosity of $8 \times 10^{39}$ erg s$^{-1}$ in 1986, but by 2019 had faded by a factor of nearly 400. It is located $0.15''$ from the center of a galaxy (SDSS J153350.89+272729) at 147 Mpc, which shows weak Type II Seyfert activity. We show that a tidal disruption event (TDE) is the preferred scenario for FIRST J153350.8+272729, although it could plausibly be interpreted as the afterglow of a long-duration $\gamma$-ray burst. This is only the second TDE candidate to be first discovered at radio wavelengths. Its luminosity fills a gap between the radio afterglows of sub-relativistic TDEs in the local universe, and relativistic TDEs at high redshifts. The unusual properties of FIRST J153350.8+272729 (ongoing nuclear activity in the host galaxy, high radio luminosity) motivate more extensive TDE searches in untargeted radio surveys.

*Keywords:* AGN host galaxies — black hole physics — radio transient sources — time domain astronomy

## 1. INTRODUCTION

The ongoing Karl G. Jansky Very Large Array (VLA) Sky Survey (VLASS; Lacy et al. 2020) is the first radio all-sky survey that is sensitive to several classes of slowly evolving extragalactic radio transients, including flares from active galactic nuclei (AGN), core-collapse supernova afterglows, the orphan afterglows of off-axis $\gamma$-ray bursts, and tidal disruption events (TDEs) of stars by supermassive black holes (SMBHs). VLASS is an interferometric survey in the 2–4 GHz band of the entire 33,885 deg$^2$ of sky north of a declination of $-40°$, with an angular resolution of $2.5''$. When complete, the sky will be surveyed over three epochs spaced by 32 months, to a continuum-image rms of 120 $\mu$Jy per beam per epoch. The exceptional survey grasp of VLASS provides the opportunity to assemble samples of radio transients without the need for external triggers, enabling radio-selected populations to be compared with those from other wavelengths.

Here we report on a remarkable radio transient discovered by jointly searching the first half of the first epoch of VLASS (VLASS 1.1) and the VLA Faint Images of the Radio Sky at Twenty centimeters (FIRST) survey (Becker et al. 1995).[1] The FIRST survey was conducted at a frequency of 1.4 GHz, and covered $\sim 10,000$ deg$^2$ of the northern sky mostly between 1994 and 1999 with an angular resolution of $5''$ and a continuum-image rms of 150 $\mu$Jy per beam. We discovered a source (see §2), FIRST J153350.8+272729 (hereafter J1533+2727), which was detected in FIRST in 1995 with a flux density of 9.7 mJy, but was undetected in VLASS in 2017. Further searches of archival radio data revealed that J1533+2727 was detected in 1986 and 1987 by the Green Bank 300-foot telescope (Condon et al. 1994) at 4.85 GHz, with a mean flux density of 51 mJy. We performed multi-band observations with the VLA on 2019 May 14 that re-detected the source at a level consistent with the VLASS upper limit (§3), notably with a flux density of just 132 $\mu$Jy at 5 GHz. J1533+2727 is associated with the nucleus of a galaxy

---

[1] A similar search yielded the discovery of the luminous extragalactic radio transient FIRST J141918.9+394036 (Law et al. 2018).

(SDSS J153350.89+272729) at a (luminosity) distance of 147 Mpc (see §4). The fading of J1533+2727 by nearly a factor of 400 over 33 years at $\sim 5$ GHz is strong evidence for its transient nature, and the preferred interpretation for its origin is of a TDE (see §5).

Although nearly a hundred TDE candidates are now cataloged[2], only $\sim 10\%$ of TDEs exhibit radio emission (Alexander et al. 2020; Anderson et al. 2019). The three most distant of the radio TDEs (Sw J1644+57, Sw J2058+05, and Sw J1112-82 at redshifts of 0.35, 1.18, and 0.89 respectively) were first discovered through transient $\gamma$-ray emission corresponding to the launch of a nascent relativistic jet. The remaining radio TDEs are powered by mildly relativistic outflows that drive shocks into the circum-nuclear medium, and peak at radio luminosities that are two to three orders of magnitude below the three relativistic radio TDEs. Only one TDE candidate, CNSS J0019+00 (Anderson et al. 2019), has previously been first discovered through its radio emission. In general, the radio emission generated by extragalactic explosions (e.g., supernovae, $\gamma$-ray bursts, and TDEs) is enhanced in the presence of more energetic outflows, and denser circum-explosion material. TDEs discovered through their radio emission, rather than through X-ray or optical emission associated with accreting material, may offer a novel selection of TDE phenomena and host galaxies.

Throughout this work, we adopt the following cosmological parameters: $H_0 = 67.7\,\mathrm{km\,s^{-1}\,Mpc^{-1}}$, $\Omega_M = 0.3089$, and $\Omega_\Lambda = 0.6911$ (Planck Collaboration et al. 2016).

## 2. DISCOVERY OF J1533+2727

Two independent efforts discovered J1533+2727 by comparing catalogs of sources from VLASS 1.1 and FIRST. Each effort first generated source catalogs from the VLASS 1.1 quick-look images[3], using either the Aegean (Hancock et al. 2012, 2018) or PyBDSF (Mohan & Rafferty 2015) source finding software. Details of how the source finding algorithms were applied will be presented in future works that describe larger samples of transients (e.g., Dong et al., in prep.). Once the VLASS 1.1 source catalogs were made, we performed cross-matches between unresolved sources in the VLASS 1.1 and FIRST catalogs, with a specific focus on finding FIRST sources not present in VLASS 1.1. In one of our efforts we only considered sources with a more than 75% decrease in measured flux densities between FIRST and VLASS. In the other effort we only

considered sources detected at $> 2.3\,\mathrm{mJy}$ in FIRST and undetected in VLASS (i.e., with 3 GHz flux densities $< 0.5\,\mathrm{mJy}$), which were additionally coincident with the nuclei of spectroscopically detected galaxies in SDSS DR14 (Abolfathi et al. 2018) at redshifts $z < 0.1$. J1533+2727 was noteworthy as one of the brightest sources to pass all our selection thresholds. The position of this source in the FIRST catalog is (R.A. J2000, decl. J2000) = (15:33:50.884, +27:27:29.57), with uncertainties of $0.4''$ in each coordinate (Becker et al. 1995).

## 3. ARCHIVAL AND FOLLOW-UP RADIO OBSERVATIONS

We searched a selection of existing radio-survey catalogs and data sets for detections of J1533+2727. The results are summarized in Table 1. J1533+2727 is cataloged in the FIRST survey with a flux density of $9.7 \pm 0.1\,\mathrm{mJy}$, on an observing epoch of 1995 November 06. The source is also present in the NVSS catalog with a flux density of $9.1 \pm 0.5\,\mathrm{mJy}$ on 1995 April 16. Although the formal $3\sigma$ upper limit on the flux density of J1533+2727 in the VLASS quick-look images is $0.38\,\mathrm{mJy}$ (based on the per-pixel rms at the source location), we adopt an upper limit of $0.46\,\mathrm{mJy}$ to account for errors in the flux scale (Perley & Butler 2017). The VLASS observation epoch was 2017 October 02. We next searched the VLA archive[4] for data obtained at the position of J1533+2727, and found that this source had been observed (in a targeted observation, at the center of the primary beam) by the Cosmic Lens All-Sky Survey (CLASS; Myers et al. 2003) on 1998 May 22 at 8.46 GHz (VLA project AM0593), and by a wideband survey of sources with rising spectra between 1.4 GHz and 4.8 GHz on 2001 September 14 (VLA project AG0617). We reanalyzed these data using standard tasks from the Common Astronomy Software Applications (CASA, version 5.1.1; McMullin et al. 2007), and finding no source at the position of J1533+2727 derived the upper limits on its flux density reported in Table 1. As above, these upper limits were derived using the per-pixel rms at the source location.

The selection of J1533+2727 as a CLASS source implied that J1533+2727 is present in the Green Bank 300-foot telescope 6 cm survey catalog (GB6; Gregory et al. 1996) with a flux density in excess of 30 mJy (Myers et al. 2003) at 4.85 GHz. Indeed, the GB6 catalog lists a $51 \pm 6\,\mathrm{mJy}$ source (GB6 J1533+2728) at a position of (R.A. J2000, decl. J2000) = (15:33:49.9±0.8, +27:28:12±12), where a substantial component of the

---

[2] See http://tde.space.

[3] https://archive-new.nrao.edu/vlass/quicklook/

[4] https://archive.nrao.edu/archive/advquery.jsp

**Table 1.** Radio Observations of FIRST J153350.8+272729.

| Epoch | Survey | Frequency (GHz) | Flux density (mJy) |
|---|---|---|---|
| 1968 | Bologna | 0.408 | < 750 |
| 1974 – 1983 | Texas | 0.365 | < 1200 |
| 1983 April 2 – 21 | GBNSS | 1.4 | < 300 |
| 1986 November 6 – December 13 | GB6 | 4.85 | $65 \pm 8$ |
| 1987 September 30 – November 1 | GB6 | 4.85 | $42 \pm 8$ |
| 1987 January | GEETEE | 0.0345 | < 15000 |
| 1995 April 16 | NVSS | 1.4 | $9.1 \pm 0.5$ |
| 1995 November 65 | FIRST | 1.4 | $9.7 \pm 0.1$ |
| 1998 May 22 | CLASS | 8.46 | < 1.5 |
| 2001 September 14 | CLASS | 1.425 | < 3 |
| 2001 September 14 | CLASS | 4.86 | < 1.5 |
| 2001 September 14 | CLASS | 8.46 | < 1.5 |
| 2001 September 14 | CLASS | 22.46 | < 7.5 |
| 2006 | VLSSr | 0.074 | < 300 |
| 2010 April – 2012 March | TGSS | 0.15 | < 15 |
| 2017 October 2 | VLASS | 3 | < 0.46 |
| 2019 May 14 | 19A-470 | 1.52 | $0.36 \pm 0.03$ |
| 2019 May 14 | 19A-470 | 5 | $0.132 \pm 0.009$ |
| 2019 May 14 | 19A-470 | 7 | $0.100 \pm 0.009$ |

NOTE—All upper limits are at the $3\sigma$ level. References: Bologna Sky Survey (Bologna; Colla et al. 1972), Texas Survey of Radio Sources at 365 MHz (Texas; Douglas et al. 1996), Green Bank Northern Sky Survey (GBNSS; White & Becker 1992), Green Bank 6 cm survey (GB6; Gregory et al. 1996), Gauribidanur Telescope (GEETEE; Dwarakanath & Udaya Shankar 1990), Faint Images of the Radio Sky at Twenty centimeters (FIRST; Becker et al. 1995), NRAO VLA Sky Survey (NVSS; Condon et al. 1998), Cosmic Lens All-Sky Survey (CLASS; Myers et al. 2003), VLA Low-frequency Sky Survey (VLSSr; Lane et al. 2014), TIFR GMRT Sky Survey Alternative Data Release (TGSS; Intema et al. 2017), VLA Sky Survey (VLASS; Lacy et al. 2020).

error is due to pointing errors of order $8''$ (Gregory et al. 1996). Despite the $46.8''$ offset between the FIRST and GB6 sources, the association is considered likely as the next closest source in FIRST or VLASS to the GB6 position is offset by $379''$, which is greater than the 3.5 arcmin full-width half-maximum of the GB6 survey beam.[5] The GB6 survey catalog is actually comprised of observations obtained over two epochs, between 1986 November 6 and December 13, and between 1987 September 30 and December 1.[6] Single epoch maps were converted into source catalogs by Gregory et al. (2001)[7]. The 1986 observations contain J1533+2727

[5] The final CLASS sample was chosen by associating GB6 sources with NVSS sources within a $70''$ separation cut, which is explained by the much greater positional uncertainty of NVSS than FIRST.

[6] Survey operations in late 1988 with the 300-foot telescope were increasingly affected by pointing errors that rendered the data unusable.

[7] Currently available at https://phas.ubc.ca/~gregory/RadioAstronomy.html.

with a flux density of $65 \pm 8$ mJy, and the 1987 observations showed a flux density of $42 \pm 8$ mJy.

The remarkable fading of J1533+2727 over 31 years between 1986 and 2017 motivated follow-up VLA observations (VLA program 19A-470). We obtained data in the B configuration (antenna separations between $0.21$ km and $11.1$ km) on 2019 May 14 in the L (1–2 GHz) and C (4–8 GHz) bands, using standard continuum observing setups and CASA data-reduction procedures. The absolute flux-scale and bandpass calibrator was 3C286, and time-variable complex gain calibration was accomplished using J1513+2338. No self-calibration was conducted. We detected J1533+2727 in both bands at a position consistent with the FIRST position within $0.2''$. The measured flux densities were $0.36 \pm 0.03$ mJy at 1.52 GHz, $0.132 \pm 0.009$ mJy at 5 GHz, and $0.100 \pm 0.009$ mJy at 7 GHz. The measurements are consistent with a single power law (flux density $S(\nu) \propto \nu^{\alpha}$, where $\nu$ is the frequency) with spectral index $\alpha = -0.840 \pm 0.003$. These measurements do not include a 3–5% uncertainty in the VLA flux-density scale (Perley & Butler 2017).

## 4. HOST-GALAXY PROPERTIES

The centroid of the FIRST position of J1533+2727 is located $0.150''$ from the optical center of the galaxy SDSS J153350.89+272729. With a FIRST positional uncertainty of $0.400''$, J1533+2727 is therefore consistent with being coincident with the galaxy nucleus. Figure 1 shows the SDSS DR16 (Ahumada et al. 2020) image and spectrum of this galaxy, which we adopt as the host of J1533+2727. The host galaxy lies at a redshift of $z = 0.03243 \pm 0.00001$ (luminosity distance of $147.14 \pm 0.01$ Mpc), and the difference between the radio position of J1533+2727 and the center of light of the host galaxy corresponds to a projected separation of just 107 pc. An inspection of the SDSS optical spectrum indicates weak Type II Seyfert activity, according to standard line-ratio diagnostics (Kewley et al. 2019), with $\log\left([NII]/H\alpha\right) = -0.05$ and $\log\left([OIII]/H\beta\right) = 0.78$. Stellar population synthesis fits to the SDSS photometry indicate a stellar mass of between $10^{10.45} M_\odot$ and $10^{10.49} M_\odot$, and an ongoing star-formation rate of $\sim 0.6 M_\odot \, \mathrm{yr}^{-1}$ ('stellarMassFSPSGranEarlyDust' table; Ahn et al. 2014). The quoted uncertainties are purely statistical, and do not reflect the range of possible parameterizations. The galaxy was classified morphologically as a spiral by Kuminski & Shamir (2016).

The absolute rest frame magnitudes of the bulge in the $g$ and $r$ bands were calculated by Simard et al. (2011) using Galaxy IMage 2D (Simard 2010), assuming extinction values obtained from the SDSS database. We transformed these bulge absolute magnitudes, $M_{g,bulge} = -18.52$ and $M_{r,bulge} = -19.39$ to the V band, $M_{V,bulge} = -19.04$, according to formulas from Jester et al. (2005). We then applied the relation between SMBH mass and bulge luminosity from McConnell & Ma (2013) to estimate the total black hole mass to be $\log M_{BH}/M_\odot = 7.6 \pm 0.2$.

## 5. DISCUSSION

### 5.1. *The nature of J1533+2727*

We now interpret these observations in terms of three hypotheses for J1533+2727:

- AGN variability.

- An engine-driven transient associated with a supernova.[8]

- A jet or outflow powered by a TDE.

---

[8] We do not consider standard supernovae because the peak radio luminosity of J1533+2727 ($1.6 \times 10^{30} \, \mathrm{erg \, s^{-1} \, Hz^{-1}}$) is a factor of eight greater than even the most luminous radio supernova (PTF 11qcj; Palliyaguru et al. 2019).

We first augment the observations presented above with archival ROSAT/PSPC pointings that included J1533+2727 in the field of view. We highlight two observations in particular: a 415 s pointing on MJD 48102 (1990 July 30; sequence id rs931238n00; around three years after the last Green Bank detection) obtained as part of the ROSAT All-Sky Survey, and a 13932 s pointing a year later on MJD 48449 (1991 July 12; sequence id RP201103N00) obtained as part of a long exposure on $\alpha$ Cor Bor. We used the `sosta` tool in the `XIMAGE` package, and the exposure maps associated with the observations, to derive $3\sigma$ upper limits on the count rates at the position of J1533+2727. These were $0.125 \, \mathrm{cts \, s^{-1}}$ and $0.0108 \, \mathrm{cts \, s^{-1}}$ on the respective dates (in the standard PSPC 0.1–2.4 keV band). We then converted these to upper limits on the 2–10 keV luminosity assuming a photon index of 2, and a Galactic neutral-hydrogen column density of $n_H = 2.9 \times 10^{20} \, \mathrm{cm^{-2}}$ derived from the HI4PI neutral hydrogen column map (HI4PI Collaboration et al. 2016). These upper limits were $L_X < 3.0 \times 10^{42} \, \mathrm{erg \, s^{-1}}$ and $L_X < 2.6 \times 10^{41} \, \mathrm{erg \, s^{-1}}$ on the respective dates.

These X-ray upper limits are low in comparison with the radio luminosity of J1533+2727, if J1533+2727 represents an active black hole. The black hole fundamental plane relates the mass, 5 GHz radio luminosity, and 2–10 keV X-ray luminosity of actively accreting objects across nine orders of magnitude in black hole mass, and hints at a fundamental link between accretion rate and jet power. We used the latest iteration of this relation (Gültekin et al. 2019) to derive predicted upper limits on the 5 GHz radio luminosity of J1533+2727 at the epochs of the X-ray observations. Given the derived SMBH mass, by assuming Poisson statistics for the X-ray upper limits, and by using a Monte Carlo technique to account for the uncertainty and intrinsic scatter in the black hole fundamental plane, we calculated 95% confidence upper limits on the expected radio luminosity of $4.8 \times 10^{38} \, \mathrm{erg \, s^{-1}}$ and $9.8 \times 10^{37} \, \mathrm{erg \, s^{-1}}$ corresponding to the two X-ray observations. These in turn imply radio flux-density upper limits of 3.7 mJy and 0.8 mJy respectively, where we divided the luminosities by the frequency to derive the spectral luminosities following Gültekin et al. (2019). If J1533+2727 was indeed this faint during the X-ray observations, a much more rapid evolution is implied between the Green Bank 4.85 GHz detection and these epochs than at later times. Furthermore, unless the source re-brightened between the X-ray observations and the NVSS and FIRST detections, an unrealistic spectral index steeper than $-2$ is implied between 1.4 GHz and 5 GHz for the FIRST detection. We conclude that J1533+2727 was inconsistent
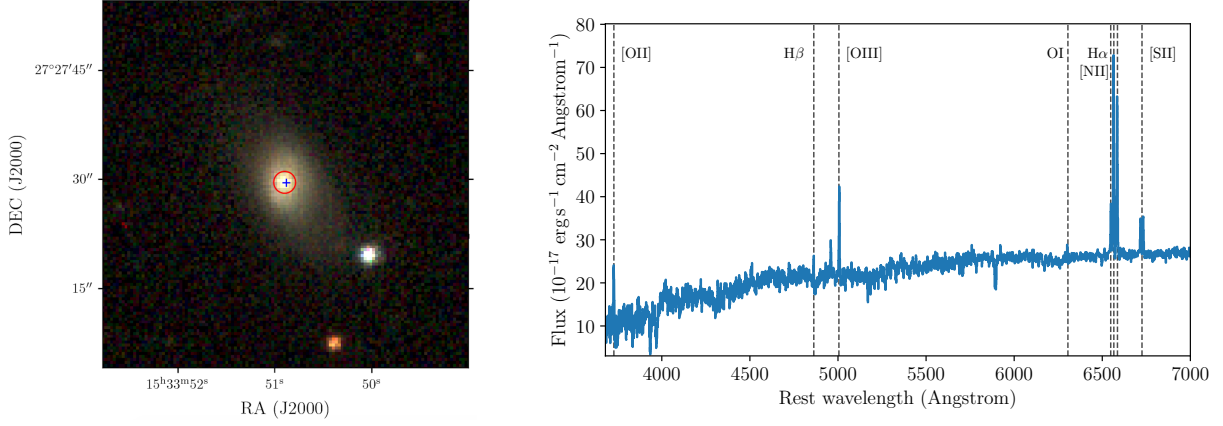
**Figure 1.** *Left:* Three-color composite in the SDSS $g$, $r$ and $i$ bands of the host galaxy of J1533+2727, SDSS J153350.89+272729. The radio position of J1533+2727 is shown as a blue cross, and the spatial extent of the SDSS fiber input on the sky is shown as a red circle (Smee et al. 2013). *Right:* SDSS spectrum (Ahumada et al. 2020) of SDSS J153350.89+272729 obtained on 2007 March 21. Some relevant emission lines are labeled, which are indicative of weak Type II Seyfert activity.

with the black hole fundamental plane when the ROSAT X-ray observations were undertaken.

This suggests that J1533+2727 was not actively accreting as an AGN at this time, which is in tension with the hypothesis of ongoing AGN variability. This is however not in tension with the TDE hypothesis, because the accretion could have ceased (e.g., Levan et al. 2016). When detected in the Green Bank survey, J1533+2727 was also more luminous at a wavelength of 6 cm than the cores of any of the 52 nearby Seyfert galaxies observed by Ho & Ulvestad (2001), besides Perseus A (NGC 1275; Seyfert 1.5) and NGC 1167 (Seyfert II; beyond the magnitude-completeness limit of the survey). Additionally, J1533+2727 is likely more variable than any of the 12 Seyferts observed by Mundell et al. (2009), within whose sample the maximum variability in seven years at 8.4 GHz was a factor of three. We therefore proceed to consider hypotheses (2) and (3) given above.

Some insight can be gained by analyzing J1533+2727 as a synchrotron transient, despite the lack of detailed spectral information. That J1533+2727 represents synchrotron emission is evident given the brightness temperature ($\gtrsim 5.3 \times 10^9$ K) implied by the extreme variability of the source.[9] We can also derive rough constraints on the source radius, $R$, the energy required to power the source, $E$, and the electron number density, $n_e$, of the medium into which the source is expanding. The constraints are based on a fiducial 65 mJy maximum

flux density measured at 4.85 GHz, and the assumption that the optically thin spectral index observed in our 2019 observations of the source of $\alpha = -0.84$ is representative of a non-evolving relativistic electron energy distribution $N(E) \propto E^{-p}$ with $p = -2\alpha + 1 = 2.68$. In the following, we assume ($a$) equipartition between the energy in relativistic electrons and in magnetic fields within the source, ($b$) that the source is expanding sub-relativistically, ($c$) that the source is spherically symmetric with a filling factor of unity, and ($d$) that the relativistic electrons are accelerated in a strong (forward) shock that deposits 10% of its energy in the electrons, and 10% of its energy in magnetic fields (i.e., $\epsilon_e = \epsilon_B = 0.1$ in usual terms).[10] The non-relativistic assumption further implies that the spectral peak was associated with synchrotron self-absorption rather than the minimum relativistic-electron energy (e.g., Chevalier 1998).

In this scenario, following Chevalier (1998), $R \propto S_p^{(p+6)/(2p+13)} \nu_p^{-1}$, and $E \propto S_p^{(3p+14)/(2p+13)} \nu_p^{-1}$, where $\nu_p$ is the peak frequency and $S_p$ is the peak flux density. If we are simply constraining the values of $R$ and $E$ when $\nu_p = 4.85$ GHz, we are setting lower limits on both quantities. This is also essentially the case if we are constraining the values of $R$ and $E$ during the 1986 Green Bank observations.[11] The electron number density is derived by applying the Rankine-Hugoniot jump conditions in the strong shock limit (Equation (15) of Ho

---

[9] A useful working definition of a variability timescale that can be used to calculate a light-crossing time is a timescale over which the modulation index, defined as the variability range divided by the mean source flux density, is greater than unity. Adopting a timescale of six years (between the FIRST/NVSS observations and L-band VLA observations in 2001), we find a brightness temperature in excess of $5.3 \times 10^9$ K.

[10] In our calculation, we adopt $c_5 = 9.68 \times 10^{-24}$ and $c_6 = 8.10 \times 10^{-41}$ from Pacholczyk (1970).

[11] If the spectrum was optically thick and $\nu_p > \nu = 4.85$ GHz, $S_p \propto (\nu_p/\nu)^2$ implies a nearly fixed estimate of $R$ regardless of the true value of $\nu_p$, and a larger value of $E$. If the spectrum was optically thin, $R$ and $E$ would clearly both be larger.

et al. 2019), with the further assumption of the shock velocity being given by the source size divided by its lifetime, $T$. In this case, $n_e \propto S_p^{-(2p+16)/(2p+13)} \nu_p^4$. In summary, using the 1986 measurement, we find

$$R = 2.3 \times 10^{17} \left( \frac{S_p}{65 \, \mathrm{mJy}} \right)^{0.47} \left( \frac{\nu_p}{4.85 \, \mathrm{GHz}} \right)^{-1} \mathrm{cm} \tag{1}$$

$$E = 7.5 \times 10^{50} \left( \frac{S_p}{65 \, \mathrm{mJy}} \right)^{1.20} \left( \frac{\nu_p}{4.85 \, \mathrm{GHz}} \right)^{-1} \mathrm{erg} \tag{2}$$

$$n_e = \frac{1.6 \times 10^{-3} \left( \frac{S_p}{65 \, \mathrm{mJy}} \right)^{-1.16} \left( \frac{T}{1 \, \mathrm{day}} \right)^2}{\left( \frac{\nu_p}{4.85 \, \mathrm{GHz}} \right)^4} \mathrm{cm}^{-3}. \tag{3}$$

These equations, including the constants of proportionality, directly reproduce Equations (8), (12), and (16) of Ho et al. (2019), for our value of $p$. Although the radius estimate is only mildly sensitive to the assumptions above, a departure from equipartition like that observed for Sw J1644+57 (Eftekhari et al. 2018), where $\epsilon_B = 0.001$ was inferred assuming $\epsilon_e = 0.1$, would increase the energy estimate by two orders of magnitude.

These results provide evidence that J1533+2727 represents a relativistic jet/outflow from a TDE. First, the lower limit on the energy in the outflow is greater than that of any known stellar cataclysm (e.g., Mattila et al. 2018) besides classical, on-axis long gamma-ray bursts (LGRBs).[12] Additionally, most LGRBs have apparent expansion velocities of $\Gamma \beta \gtrsim 3$ (here, $\Gamma$ is the bulk Lorentz factor of the emitting material, and $\beta = v/c$ is the normalized expansion velocity). However for J1533+2727, following Sari et al. (1998), the characteristic frequency corresponding to radiation from the lowest-energy relativistic electrons, $\nu_m$, was likely lower than 4.85 GHz in 1986, because the source declines between 1986 and 1987. This frequency is related to $E$ and $T$ in the case of adiabatic evolution, which implies a lifetime:

$$T \gtrsim 22 \left( \frac{E}{7.5 \times 10^{50} \, \mathrm{erg}} \right)^{1/2} \mathrm{days}. \tag{4}$$

This in turn implies $\Gamma \beta \lesssim 4$, and $n_e \lesssim 0.8 \, \mathrm{cm}^{-3}$. Although this makes the LGRB scenario somewhat fine-tuned, the derived parameters are consistent with some

---

[12] Radio calorimetry of the ejecta of cosmic explosions traces the fastest ejecta, and therefore cannot be directly related to the total energies in outflows with a range of velocities, like supernovae (e.g., Berger et al. 2003).

GRBs (e.g., GRB 980703; Perley et al. 2017). Indeed, GRB 980703 exhibits late-time emission 16 years post-burst that is similar to J1533+2727 (Perley et al. 2017). However, the projected offset between J1533+2727 and the center of light of its host galaxy of $\approx 100 \, \mathrm{pc}$ is inconsistent with more than 95% of the LGRB population (Lyman et al. 2017). Additionally, the high stellar mass and lack of evidence for an ongoing starburst in the host galaxy of J1533+2727 are inconsistent with typical LGRB hosts (Taggart & Perley 2019). We therefore favor the TDE scenario.

A comparison between the radio lightcurve of J1533+2727 and the remainder of the TDE population is shown in Figure 2. The post-explosion time of the 1986 epoch (88 days) was derived assuming a nominal expansion velocity of $c$, which would imply $n_e \sim 12 \, \mathrm{cm}^{-3}$. Please note however that sub-relativistic expansion was assumed to derive the constraints above, and this is therefore for illustrative purposes only. The high radio luminosity and outflow energy relative to several radio-detected TDEs is suggestive of a relativistic jet, rather than a wide-angle outflow (Alexander et al. 2020). We note that if the emission region were significantly aspherical, with a non-unity filling factor, some of the above conclusions would be altered by factors of a few (Barniol Duran et al. 2013).

## 5.2. *Implications for the TDE population*

We have established that J1533+2727 is a remarkable radio transient and a likely TDE afterglow. Using the FIRST survey, and assuming the detection of just one such source, we can calculate a lower limit on the occurrence of sources like J1533+2727. The 1 mJy minimum flux density of the FIRST catalog and the peak luminosity of J1533+2727 in FIRST implies a detectable distance of 452 Mpc. The FIRST and VLASS 1.1 sky surveys have an overlapping sky coverage of $\sim 6000 \, \mathrm{deg}^2$, and thus the detectable distance corresponds to an observable volume of $0.056 \, \mathrm{Gpc}^3$. J1533+2727 emitted above its detected FIRST luminosity for at least 8 years between the Green Bank and FIRST detections. We can therefore infer a lower limit on the volumetric rate of approximately $2.2 \, \mathrm{Gpc}^{-3} \mathrm{yr}^{-1}$, or $\sim 1\%$ of the observed TDE rate (van Velzen 2018). We do not take this analysis further because the search for TDEs detected in FIRST is ongoing.

Our results add to the emerging picture of the diversity of TDE-driven jets/outflows from supermassive black holes. Although it has long been known that $\sim 50\%$ of the mass of a disrupted star is likely to be unbound (e.g., Rees 1988), the geometry and kinematics of such outflows are poorly constrained, as are any
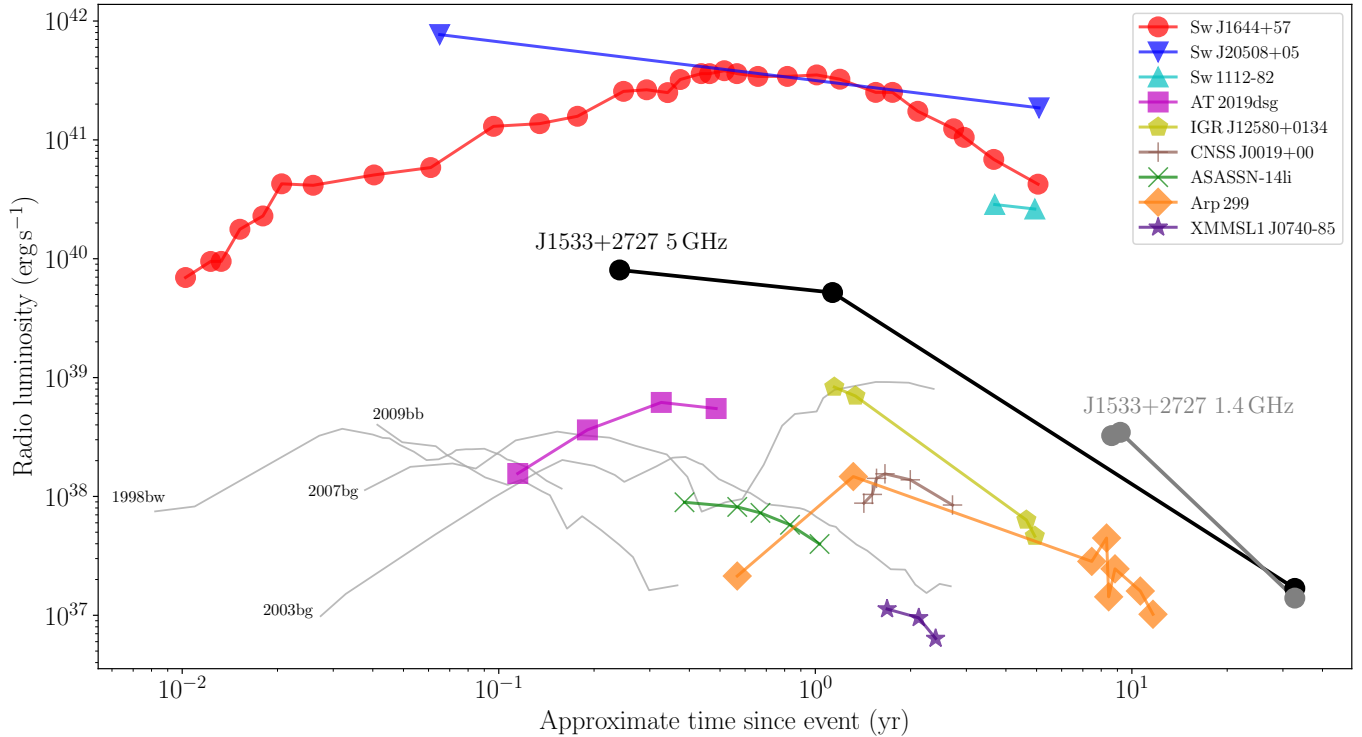
**Figure 2.** Lightcurves of all TDEs detected at radio wavelengths. All TDE data are at 5 GHz, except for the 1.4 GHz data on J1533+2727, and 8.4 GHz data on AT2019dsg and Arp 299. Data were collated from Alexander et al. (2020) and references therein. The time since the event for the first data point on J1533+2727 (88 days) was derived assuming expansion at the speed of light to that time (see text for details). Also shown are representative radio lightcurves of four luminous supernovæ: the relativistic-outflow events 1998bw (4.8 GHz; Kulkarni et al. 1998) and 2009bb (8.46 GHz; Soderberg et al. 2010), and the energetic Type Ic broad line events 2003bg (8.5 GHz; Soderberg et al. 2006) and 2007bg (8.5 GHz; Salas et al. 2013). In the latter two supernovae the late-time radio emission was enhanced by a dense, structured circumstellar medium.

jets/outflows powered by the accretion of the remaining 50% of the mass. The radio luminosity and derived outflow energy of J1533+2727 fills the gap between the three relativistic TDEs identified through their prompt high-energy emission, and the remaining TDE sample (Figure 2). The host galaxy of J1533+2727 and its central supermassive black hole appear otherwise unremarkable with respect to the TDE population (French et al. 2020; Wevers et al. 2017). Although the black hole mass is somewhat high relative to optically selected TDEs (Wevers et al. 2017), stars with a wide range of masses ($\gtrsim 0.3 M_\odot$) are expected to be disrupted by such black holes (Kochanek 2016). The optical spectrum of the host of J1533+2727 shows emission lines characteristic of the narrow-line regions of Type II Seyferts; this nuclear activity must have been ongoing prior to the transient event, given the large expected sizes of narrow-line regions (e.g. Bennert et al. 2006). This is similar to the host of the radio-discovered TDE CNSS J0019+00 (Anderson et al. 2019). The presence of nuclear activity in the spectrum of the J1533+2727 host makes it difficult to determine whether or not it

is a post-starburst galaxy, although we note that TDEs are found to be over-represented in galaxies that are evidently post-starburst from their optical spectra (Figure 3; French et al. 2016, 2020). We speculate that TDEs discovered in radio transient surveys will have substantially different selection effects, especially with regards to AGN activity and extinction, than the selection effects present in optical and soft X-ray surveys that dominate TDE discoveries today.

## 6. CONCLUSIONS

We present the discovery of the candidate TDE FIRST J153350.8+272729 using the GB6, FIRST, and VLASS radio surveys. The source was first detected in 1986 with a flux density of 65 mJy at 4.85 GHz, and has been monotonically fading ever since. This is the second TDE candidate to be solely identified at radio wavelengths. Its radio luminosity (observed maximum of $8 \times 10^{39}$ erg s$^{-1}$), and the implied energy in the outflow generated by the TDE ($\gtrsim 7 \times 10^{50}$ erg), fill a gap between most radio-detected TDEs and the three high-redshift events that were first discovered through their prompt $\gamma$-ray emission. Little more can be said about
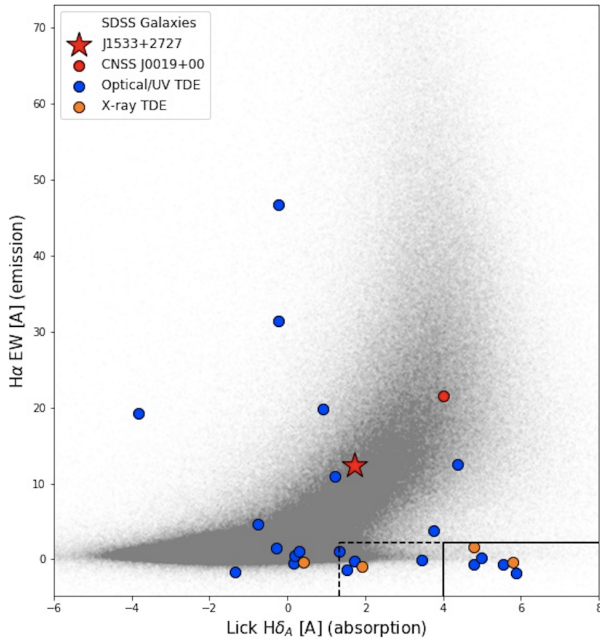
**Figure 3.** Plot adapted from French et al. (2020) (their Figure 5 – see French et al. (2020) and French et al. (2016) for details) showing spectral indices of a sample of SDSS galaxies, and selected TDE hosts including J1533+2727. Hα emission traces current star formation while Hδ absorption traces star-formation activity in the past ∼Gyr. Post-starburst / quiescent Balmer-strong galaxies comprising 0.2% (solid box) and 2% (dashed box) of the parent SDSS sample are at the lower right of the plot. The hosts of optically and X-ray selected TDEs are over-represented among post-starburst galaxies. Although only two radio-selected TDE candidates have been identified so far (J1533+2727 and CNSS J0019+00), neither is hosted by a post-starburst galaxy.

the nature of the outflow and the medium into which it propagates, because we have only observed the optically thin component of the radio spectral energy distribution. The host galaxy, at a distance of 147 Mpc, is largely unremarkable (inferred supermassive black hole mass of $4 \times 10^7 M_\odot$), and shows signatures of Type II Seyfert activity. We anticipate that ongoing surveys for radio transients like VLASS, and with the Australian Square Kilometre Array Pathfinder (Murphy et al. 2013), and the Aperture Tile In Focus at the Westerbork Synthesis Radio Telescope (Oosterloo et al. 2009), together with dedicated radio follow-up observations will yield several such TDEs that may help untangle selection effects in surveys in other bands.

REFERENCES

Abolfathi, B., Aguado, D. S., Aguilar, G., et al. 2018, ApJS, 235, 42

Ahn, C. P., Alexandroff, R., Allende Prieto, C., et al. 2014, ApJS, 211, 17

Ahumada, R., Allende Prieto, C., Almeida, A., et al. 2020, ApJS, 249, 3

Alexander, K. D., van Velzen, S., Horesh, A., & Zauderer, B. A. 2020, SSRv, 216, 81

Anderson, M. M., Mooley, K. P., Hallinan, G., et al. 2019, arXiv e-prints, arXiv:1910.11912

Barniol Duran, R., Nakar, E., & Piran, T. 2013, ApJ, 772, 78

Becker, R. H., White, R. L., & Helfand, D. J. 1995, ApJ, 450, 559

Bennert, N., Jungwiert, B., Komossa, S., Haas, M., & Chini, R. 2006, A&A, 456, 953

Berger, E., Kulkarni, S. R., Frail, D. A., & Soderberg, A. M. 2003, ApJ, 599, 408

Chevalier, R. A. 1998, ApJ, 499, 810

Colla, G., Fanti, C., Fanti, R., et al. 1972, A&AS, 7, 1

Condon, J. J., Broderick, J. J., Seielstad, G. A., Douglas, K., & Gregory, P. C. 1994, AJ, 107, 1829

Condon, J. J., Cotton, W. D., Greisen, E. W., et al. 1998, AJ, 115, 1693

Douglas, J. N., Bash, F. N., Bozyan, F. A., Torrence, G. W., & Wolfe, C. 1996, AJ, 111, 1945

Dwarakanath, K. S., & Udaya Shankar, N. 1990, JAA, 11, 323

Eftekhari, T., Berger, E., Zauderer, B. A., Margutti, R., & Alexander, K. D. 2018, ApJ, 854, 86

French, K. D., Arcavi, I., & Zabludoff, A. 2016, ApJL, 818, L21

French, K. D., Wevers, T., Law-Smith, J., Graur, O., & Zabludoff, A. I. 2020, SSRv, 216, 32

Graur, O. 2018, arXiv e-prints, arXiv:1809.08078

Gregory, P. C., Capak, P., Gasson, D., & Scott, W. K. 2001, in IAU Symposium, Vol. 205, Galaxies and their Constituents at the Highest Angular Resolutions, ed. R. T. Schilizzi, 98

Gregory, P. C., Scott, W. K., Douglas, K., & Condon, J. J. 1996, ApJS, 103, 427

Gültekin, K., King, A. L., Cackett, E. M., et al. 2019, ApJ, 871, 80

Hancock, P. J., Murphy, T., Gaensler, B. M., Hopkins, A., & Curran, J. R. 2012, MNRAS, 422, 1812

Hancock, P. J., Trott, C. M., & Hurley-Walker, N. 2018, PASA, 35, e011

HI4PI Collaboration, Ben Bekhti, N., Flöer, L., et al. 2016, A&A, 594, A116

Ho, A. Y. Q., Phinney, E. S., Ravi, V., et al. 2019, ApJ, 871, 73

Ho, L. C., & Ulvestad, J. S. 2001, ApJS, 133, 77

Intema, H. T., Jagannathan, P., Mooley, K. P., & Frail, D. A. 2017, A&A, 598, A78

Jester, S., Schneider, D. P., Richards, G. T., et al. 2005, AJ, 130, 873

Kewley, L. J., Nicholls, D. C., & Sutherland, R. S. 2019, ARA&A, 57, 511

Kochanek, C. S. 2016, MNRAS, 461, 371

Kulkarni, S. R., Frail, D. A., Wieringa, M. H., et al. 1998, Nature, 395, 663

Kuminski, E., & Shamir, L. 2016, VizieR Online Data Catalog, 222

Lacy, M., Baum, S. A., Chandler, C. J., et al. 2020, PASP, 132, 035001

Lane, W. M., Cotton, W. D., van Velzen, S., et al. 2014, MNRAS, 440, 327

Law, C. J., Gaensler, B. M., Metzger, B. D., Ofek, E. O., & Sironi, L. 2018, ApJL, 866, L22

Levan, A. J., Tanvir, N. R., Brown, G. C., et al. 2016, ApJ, 819, 51

Lyman, J. D., Levan, A. J., Tanvir, N. R., et al. 2017, MNRAS, 467, 1795

Mattila, S., Pérez-Torres, M., Efstathiou, A., et al. 2018, Science, 361, 482

McConnell, N. J., & Ma, C.-P. 2013, ApJ, 764, 184

McMullin, J. P., Waters, B., Schiebel, D., Young, W., & Golap, K. 2007, in Astronomical Society of the Pacific Conference Series, Vol. 376, Astronomical Data Analysis Software and Systems XVI, ed. R. A. Shaw, F. Hill, & D. J. Bell, 127

Mohan, N., & Rafferty, D. 2015, PyBDSF: Python Blob Detection and Source Finder, , , ascl:1502.007

Mundell, C. G., Ferruit, P., Nagar, N., & Wilson, A. S. 2009, ApJ, 703, 802

Murphy, T., Chatterjee, S., Kaplan, D. L., et al. 2013, PASA, 30, e006

Myers, S. T., Jackson, N. J., Browne, I. W. A., et al. 2003, MNRAS, 341, 1

Oosterloo, T., Verheijen, M. A. W., van Cappellen, W., et al. 2009, in Wide Field Astronomy & Technology for the Square Kilometre Array, 70

Pacholczyk, A. G. 1970, Radio astrophysics. Nonthermal processes in galactic and extragalactic sources

Palliyaguru, N. T., Corsi, A., Frail, D. A., et al. 2019, ApJ, 872, 201

Perley, D. A., Hjorth, J., Tanvir, N. R., & Perley, R. A. 2017, MNRAS, 465, 970

Perley, R. A., & Butler, B. J. 2017, ApJS, 230, 7

Planck Collaboration, Ade, P. A. R., Aghanim, N., et al. 2016, A&A, 594, A13

Rees, M. J. 1988, Nature, 333, 523

Salas, P., Bauer, F. E., Stockdale, C., & Prieto, J. L. 2013, MNRAS, 428, 1207

Sari, R., Piran, T., & Narayan, R. 1998, ApJL, 497, L17

Simard, L. 2010, GIM2D: Galaxy IMage 2D, Astrophysics Source Code Library, , , ascl:1004.001

Simard, L., Mendel, J. T., Patton, D. R., Ellison, S. L., & McConnachie, A. W. 2011, 196, 11

Smee, S. A., Gunn, J. E., Uomoto, A., et al. 2013, AJ, 146, 32

Soderberg, A. M., Chevalier, R. A., Kulkarni, S. R., & Frail, D. A. 2006, ApJ, 651, 1005

Soderberg, A. M., Chakraborti, S., Pignata, G., et al. 2010, Nature, 463, 513

Taggart, K., & Perley, D. 2019, arXiv e-prints, arXiv:1911.09112

van Velzen, S. 2018, ApJ, 852, 72

Wevers, T., van Velzen, S., Jonker, P. G., et al. 2017, MNRAS, 471, 1694

White, R. L., & Becker, R. H. 1992, ApJS, 79, 331